ELECTRONIC DEFECTS IN CdSe NANOCRYSTALS EMBEDDED IN GeS$_2$ AMORPHOUS MATRIX

Z. Aneva[*], D. Nesheva, C. Main[a], S. Reynolds[b]

Institute of Solid State Physics, Bulgarian Academy of Sciences, 72 Tzarigradsko Chaussee Blvd., 1784 Sofia, Bulgaria
[a]University of Dundee, Faculty of Engineering and Physical Sciences, Dundee DD1 4HN, UK
[b]Institute of Photovoltaics, Forschungszentrum Jülich, 52425 Jülich, Germany

Electronic defects in CdSe nanocrystals of a-GeS$_2$/nc-CdSe superlattices and composite films are investigated and compared with results obtained for similar SiO$_x$/CdSe films. A wide band of localized states centred at 0.55 eV below the conduction band edge is seen in both groups of samples and identified with defects in the nanocrystal bulk. A band at ~ 0.7 eV below the conduction band is well resolved in SiO$_x$/CdSe samples but not seen in GeS$_2$/CdSe films. As this feature is ascribed to defects at the CdSe-CdSe interface, a lower density of such defects is assumed in the latter case. In GeS$_2$/CdSe samples a new band located at 0.50 eV below the conduction band appears. It is attributed to defects at the GeS$_2$-CdSe interface. Optical absorption measurements reveal that defect concentration above the valence band of CdSe nanocrystals in GeS$_2$/CdSe samples is lower than in SiO$_x$/CdSe ones. Steady-state photoconductivity of GeS$_2$/CdSe samples shows that at low temperatures the mobility-lifetime product in CdSe nanocrystals decreases with decreasing nanocrystal size. This observation is related to deep defects at the interface of CdSe nanocrystals and reflects the increasing surface to volume ratio.

1. Introduction

Interest in nanometer-sized semiconductor crystals, in particular II-VI alloys, has rapidly increased over the recent years, because of their potential applications in optoelectronics, and nonlinear optics [1]. In contrast to bulk crystals, a large fraction of the constituent atoms are located at the surface of isolated nanocrystals or within the grain boundaries of nanometer-sized composite or polycrystalline materials. This leads to a variety of defects (dangling and wrong bonds, bond lengths longer or shorter than those in the bulk, surface oxidation etc.) and significantly affects electrical and optical properties of nanosized semiconductors [2]. Photo- and electroluminescence, carrier dynamics etc., strongly depend on the states at the interface with the surrounding media [3-5]. Therefore, studies of the energy distribution and concentration of defect states in the gap, which are connected with crystallite size, composition and the preparation conditions are of interest from both fundamental and practical points of view.

In this study optoelectronic properties of GeS$_2$/CdSe superlattices and composite films have been investigated and are compared with those obtained for similar samples from the SiO$_x$-CdSe system. Fourier-transform transient photoconductivity (TPC) and spectral photocurrent measurements were used to probe localised states in the upper and lower portions of the band gap, respectively. Steady-state photoconductivity measurements were carried out to obtain information

---

[*] Corresponding author: zdaneva@pronto.phys.bas.bg

on carrier recombination. The influence of the matrix on the defect state distribution in CdSe nanocrystals is discussed.

2. Experimental details

Consecutive thermal evaporation of powdered CdSe (Merck, "Suprapure") and 'matrix' material (GeS$_2$ or SiO) was carried out from two independent tantalum crucibles at a vacuum of 5.10^{-4} Pa for the GeS$_2$-CdSe system and ~10^3 Pa for the SiO$_x$-CdSe system (x≈1.5) [6]. Three groups of samples were investigated: I) Superlattices (SLs) of GeS$_2$(SiO$_x$)/CdSe with equal sublayer thicknesses of 5.0 nm; II) Composite films (CFs) of GeS$_2$ (SiO$_x$)/CdSe, consisting of thin island-type layers of CdSe with nominal layer thickness of 3.0 or 5.0 nm (number of layers 28 and 16, average nanocrystal diameter of 5.0 and 6.6 nm, respectively [7,8]), sandwiched between thicker layers of GeS$_2$ (SiO$_x$), (nominal thickness ratio 1:20); III) CdSe single films deposited under the same conditions as those used in SLs and CFs preparation. The nominal film thickness and deposition rate (0.5 nm/s for CdSe, 3.5 nm/s for SiO$_x$ and 2.5 nm/s for GeS$_2$) were controlled during deposition by two calibrated quartz monitors (type MIKI-FFV). Corning 7059 glass substrates were used and were not intentionally heated. Layer by layer deposition of each sublayer in SLs was performed by rotating the substrates at rates between 8 and 15 r.p.m above the respective source. Step-by-step deposition of CdSe and one-step deposition of GeS$_2$ (SiO$_x$) was used in preparation of respective sublayers in the composite films. High-resolution electron microscopy (HREM) measurements [6, 9, 10] have shown that in the superlattices, sublayers are continuous, smooth and of uniform thickness as CdSe sublayers consist of randomly oriented nanocrystals. In the composite films CdSe sublayers are discontinuous. CdSe nanocrystals are also randomly oriented being partly isolated and partly in contact

Co-planar electrical contacts of sputtered gold (about 1 cm long and spaced 0.15 cm apart) were made on the top surface of the samples. For transient photoconductivity measurements, an electrically screened Laser Science VSL-337 N$_2$ laser plus dye attachment was used to generate 4 ns pulses of 500 nm light at a flux of 2×10^{14} cm^{-2} attenuated if required by means of neutral density filters. Following preamplification, the photocurrent decay at 300 V dc bias was recorded on a Tektronix TDS3052 storage oscilloscope and data transferred to a PC for analysis. Measurements between 100 K and 400 K were made in a screened cryostat.

Spectral photocurrent measurements were performed with chopped light (2 Hz) from a diffraction grating monochromator at a resolution of 2 nm/mm. Moddel's relation [11] $\alpha = \alpha_0(F_0/F)(I/I_o)^{1/\beta}$ was used to obtain the spectral dependence of the relative absorption coefficient α. Here F is the incident flux, I is the photocurrent and β is the power-law index of the photocurrent intensity dependence, which was found to be close to 1 for all samples used in this study. The subscript "o" refers to some known reference photon energy.

Steady-state photoconductivity measurements were carried out by Keithley 610 Electrometer in the temperature region 77 - 293 K while illuminating samples with green light (λ=525 nm, 2.5×10^{15} cm^{-2} s^{-1}). The samples were heated at a rate of ~ 0.05 K/s.

3. Results and discussion

Analysis of the TPC measurements over a range of temperatures has been made in terms of multiple-trapping, using the Fourier-transform density of states (DOS) spectroscopy [12]. The defect distribution obtained for the samples studied is shown in Fig. 1. The energy scaling of the DOS plot was carried out assuming an attempt-to-escape frequency of 1×10^{12} s^{-1}, since this gave good agreement at different temperatures. As a number of factors such as the capture cross-section of the defects and the carrier mobility must be known, the absolute scaling of the DOS is difficult to deduce and the DOS magnitudes in this study are only relative. Nevertheless, one can see significant differences in the shape of the DOS distributions for different films. These of SiO$_x$/CdSe SL and CF are rather flat (taking note of the different scales used in Fig 1) when compared with the CdSe single layer. In addition, the shape of the DOS in the CdSe single layer is quite different from that of the

SiO$_x$/CdSe CF. Moreover, a gradual change in the shape, approaching that of the CdSe film, has been observed for SiO$_x$/CdSe SLs [13] with increasing CdSe sublayer thickness. Deconvolution of the curves performed for all SiO$_x$/CdSe SLs and the '5 nm' CF showed that the DOS distribution is composed of two broad defect bands, peaked at about 0.55 eV and 0.65-0.7 eV. It has been suggested [13] that the deeper states are associated with CdSe-CdSe interface defects while the shallower ones may originate from the nanocrystal volume.
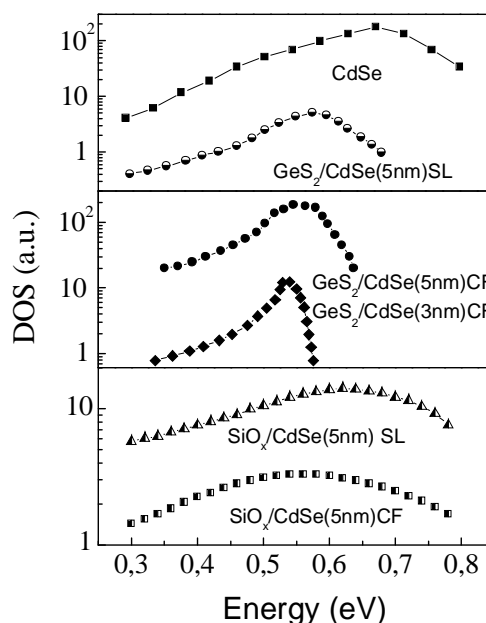

Fig.1. DOS distribution of (from top down): a CdSe single layer, a GeS$_2$/CdSe(5 nm) superlattice, '5' nm and '3' nm GeS$_2$/CdSe composite films, a SiO$_x$/CdSe(5 nm) superlattice, and a '5' nm SiO$_x$/CdSe composite film. Pay attention that the y-scale is different for different layers. Although the plots shown are only a relative measure of the DOS, they may be used to compare the magnitudes and energy positions of defects.

The DOS distribution of GeS$_2$/CdSe SLs and CFs has quite a different shape compared with the SiO$_x$/CdSe samples (see Fig.1). The wide band of localized states peaking at 0.55 eV below the conduction band edge is clearly evident in both kinds of GeS$_2$/CdSe samples, but while that at 0.65-0.7 eV may still exist in the SL, it is missing in the CFs.. This observation implies that in the GeS$_2$/CdSe samples the CdSe-CdSe interface defect density is rather low. HREM investigations of SiO$_x$/CdSe and GeS$_2$/CdSe CFs have shown [9,10] that the mechanism of CdSe nanoparticle formation on both oxide and chalcogenide surfaces is similar. Independently of the chemical nature of the surface, at the very beginning of CdSe deposition embryos are formed at surface positions at which the curvature and lattice stress are greatest. Further CdSe deposition does not create new embryos, but increases only the size of already formed nanoparticles. Based on this mechanism of CdSe nanoparticle formation, the strong reduction of CdSe-CdSe interface defect density observed in GeS$_2$-CdSe CFs can be considered as indication that the surface topology of GeS$_2$ matrix layers facilitates formation of CdSe nanocrystals which are better separated by the matrix material. This assumption is in good agreement with previous absorption and Raman scattering results [7,8]. A new broad defect band peaked at about 0.50 eV below the conduction band edge appears in the DOS distribution of the GeS$_2$/CdSe SL and GeS$_2$/CdSe CFs (see Fig.1). Since such a band has not been observed in SiO$_x$/CdSe samples, it may be related to defect states at the GeS$_2$-CdSe interface.

As already mentioned, the band at 0.55 eV, attributed to defects in the nanocrystal bulk, is observed in the DOS distribution of all samples. It is probably connected with the CdSe deposition conditions which, for example, can cause a slight stoichiometry disturbance. The energy position of

this band practically coincides with the position of double Se vacancies in CdSe monocrystals,which act as deep donors [14].
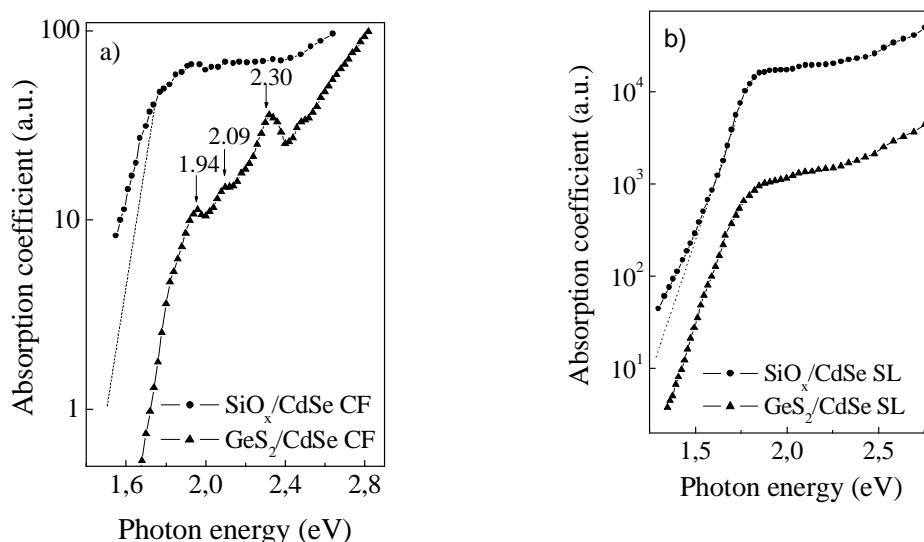

Fig.2. Optical absorption spectra of two CFs (a) and two SLs (b) having nominal CdSe layer thickness of 5 nm. The dashed lines at the spectra of SiO$_x$/CdSe CF and SL are parallel to the tails of the corresponding GeS$_2$/CdSe s amples and are shown for illustration of the difference in the Urbach tail slopes.

Absorption spectra of '5nm' GeS$_2$/CdSe and SiO$_x$/CdSe composite films are shown in Fig. 2a. They each exhibit a well pronounced exponential (Urbach) tail having a different characteristic energy E_u; in SiO$_x$/CdSe CF E_u = 85 meV while in the GeS$_2$/CdSe CF it is 61 meV. As band tailing is a characteristic measure of the degree of lattice disorder, the larger the slope of the tail, the greater the disorder in nanocrystals. Hence, the lower E_u in GeS$_2$/CdSe CF implies that GeS$_2$-CdSe interfaces do not create such a strong lattice disorder in CdSe NCs as SiO$_x$-CdSe interfaces. This observation illustrates the important effect of the matrix material on the defect state distribution in nanocrystals. Moreover, at energies higher than the optical band gap of bulk CdSe (1.75 eV), three distinct features at 1.94 eV, 2.09 eV and 2.30 eV are seen in the absorption spectrum of the GeS$_2$/CdSe CF which are not observed in the spectrum of the SiO$_x$/CdSe CF. These features have been ascribed [7] to three-dimensional carrier confinement in each separate CdSe nanocrystal. They indicate the high monodispersity and high quality of CdSe nanocrystal lattice of GeS$_2$/CdSe samples and concur with the TPC result showing a very low amplitude of the putative '0.65-0.7 eV' defect band in the DOS.

The absorption spectra of GeS$_2$/CdSe and SiO$_x$/CdSe superlattices having layer thickness of 5 nm are compared in Fig. 2b. It is seen from the figure that at the lowest energies absorption in SiO$_x$/CdSe SL deviates from the exponential tail A careful analysis of the absorption curves of SiO$_x$/CdSe superlattices with various CdSe layer thickness has indicated [15] that the thinner the CdSe layers, the shorter the exponential part of the absorption tail. The non-exponential absorption has been attributed to electronic transitions from defect levels located somewhere in the energy region of the valence band tail and conduction band bottom. An energy of more than 0.3 eV (above the top of the first mini-band of the valence band in CdSe layers) has been roughly estimated for the position of the suggested defect levels and they have been related to defect states at the SiO$_x$-CdSe interface [15]. Although E_u in GeS$_2$/CdSe superlattices (62 meV) is similar to those obtained in SiO$_x$/CdSe ones (55-60 meV), the absorption tail in the GeS$_2$/CdSe samples is exponential over a wide energy range. This indicates that, in contrast with SiO$_x$/CdSe SLs and CFs, in GeS$_2$/CdSe samples the concentration of interface defect states in the lower portions of the band gap, if they exist, is quite low. The observation could be related to the different nature of interface bonds.
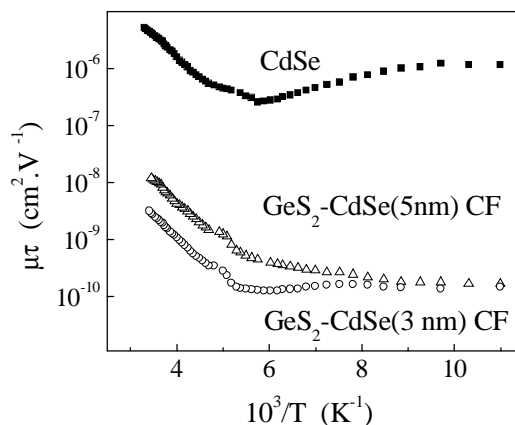
Fig. 3. Temperature dependences of the mobility-lifetime product for a CdSe single film and
3nm and 5 nm GeS$_2$/CdSe composite films.

We note that, at the same nominal thickness of CdSe sublayers, absorption tails of SiO$_x$/CdSe composite films are broader than those of superlattices, while the E_u of GeS$_2$/CdSe composite films and that of the superlattices from both systems is practically the same. This indicates that disorder in CdSe nanocrystals embedded in a SiO$_x$ matrix is higher than that in the other three kinds of samples which concurs with the above conclusion for a strong disorder effect of the SiO$_x$-CdSe interface.

Temperature dependences of the mobility-lifetime product $\mu\tau$ calculated from steady-state photoconductivity data of a CdSe single film and two GeS$_2$/CdSe CFs are shown in Fig. 3. In the case of the CdSe film a thermal quenching beginning at 110 K is observed followed by an increase at temperatures ~180 K. One can also see that $\mu\tau$ strongly decreases with decreasing CdSe crystal size. Room temperature $\mu\tau$ values of 4.0×10^{-6} cm^{2}V^{-1}, 1.2×10^{-8} cm^{2}V^{-1} and 3.1×10^{-9} cm^{2}V^{-1} have been obtained for CdSe single layer, 5 nm and 3 nm GeS$_2$/CdSe CFs, respectively. In the composite films the CdSe thickness was taken as a sum of the nominal thickness of the individual CdSe sublayers.

It is known [16] that in bulk CdSe the low-temperature photoconductivity is related to 'slow' recombination centres located at ~ 0.6 eV above the valence band, which are usually associated with Cd vacancies. Bearing in mind that the smaller the CdSe nanocrystal size, the larger the surface-to-volume ratio, one can attribute the observed strong $\mu\tau$ decrease in GeS$_2$/CdSe CFs to the presence of a high concentration of some deep interface defects that play role of 'fast' recombination centers. Similar results have been obtained in Se/CdSe SLs [17], the fast recombination centers in this case being located 0.71eV above the valence band edge of CdSe.

4. Conclusions

Density of state distributions in the upper half of the gap of continuous and discontinuous CdSe nanocrystal layers in GeS$_2$/CdSe superlattices and composite films have been explored using TPC and spectral photocurrent measurements. The DOS distribution has been compared with that obtained for SiO$_x$/CdSe samples similarly prepared. Based on the difference in the characteristic energy of the Urbach tail, it is concluded that SiO$_x$ causes stronger deformations in the CdSe nanocrystal lattice than GeS$_2$. A defect band located at 0.55 eV below the conduction band edge has been observed in all samples of both systems and related to defects in the nanocrystal volume (most likely double Se vacancies). The band at 0.65-0.7 eV, observed in SiO$_x$/CdSe samples and attributed to defects at the CdSe-CdSe interface, has not been seen in the DOS of GeS$_2$/CdSe SL and CFs. Instead a new band appears, 0.5 eV below the conduction band edge, associated with defects at the GeS$_2$-CdSe interface.

Steady-state photocurrent measurements on CdSe single films and GeS_2/CdSe CFs reveal a reduction in mobility-lifetime product as layer thickness is reduced. Given that carrier recombination is likely to proceed via deep defects, this result suggests that such defects originate at the interface of CdSe nanocrystals and reflects the increasing surface to volume ratio.

Acknowledgements

References

 [1] A. D. Yoffe, Advances in Physics **50**, 1 (2001)
 [2] S. Veprek, Thin Solid Films **297**, 145 (1997)
 [3] M. Fujii, Y. Inoue, Sh. Hayashi, K. Yamamoto, Appl. Phys. Lett. **68,** 3749 (1996)
 [4] S. Lombardo, S. Coffa, C. Bongiorno, C. Spinella. E. Castagna, A. Sciuto, C. Gerardy,
     F. Ferrari, B. Fazio, S. Privitera, Mat. Sci. Eng. B **69-70,** 295 (2000)
 [5] G. Franzo, A. Irrera, E. C. Moreira, M. Miritello, F. Iacona, D. Sanfolippo, G. DiStefano,
     P. G. Fallica, F. Priolo, Appl. Phys. A **74,** 1 (2002)
 [6] D. Nesheva, in Handbook of Surfaces and Interfaces of materials, edited H.S. Nalwa, Academic
     Press, San Diego (2001), Vol. 3, p.239.
 [7] D. Nesheva, Z. Levi, Z. Aneva, I. Zrinscak, C Main and S. Reynolds, J. Nanoscience &
     Nanotechnology **3**, 645 (2002).
 [8] C. Raptis, D. Nesheva, Y.C. Boulmetis, Z. Levi, Z. Aneva, J. Phys.: Condens. Matter
     16, 8221 (2004).
 [9] D. Nesheva, H. Hofmeister, Z. Levi and Z. Aneva, Vacuum 65, 109 (2002)
[10] D. Nesheva and H. Hofmeister, Solid State Commun. **114**, 511-514 (2000).
[11] G. Moddel, D. Anderson and W. Paul, Phys. Rev. B **22**, 1918-1925 (1980).
[12] S. Reynolds C. Main, D. P. Webb, M. J. Rose, Phil. Mag. B **80**, 547 (2000).
[13] D. Nesheva, S. Reynolds, C. Main, Z. Aneva and Z. Levi, Phys. Stat. Sol. (a) **195**, accepted.
[14] Landolt-Bornstein Numerical Data and Functional Relationships in Science and Technology,
     New Series, 1982, Editor in Chief K.-H.Hellewege (Berlin: Springer-Verlag) vol.17,
     subvolume b, p. 210.
[15] D. Nesheva, Z. Levi, Z. Aneva, V. Nikolova and H. Hofmeister, J. Phys.: Condens. Matter.
     12, 751 (2000).
[16] R. H. Bube, Photoelectronic Properties of Semiconductors, Cambridge University Press,
     Cambridge U.K. (1992).
[17] D. Nesheva, Thin Solid Films **280**, 51 (1996).